



NRC Publications Archive Archives des publications du CNRC

Accurate O–H bond dissociation energy differences of hydroxylamines determined by EPR Spectroscopy: computational insight into stereoelectronic effects on BDEs and EPR spectral parameters

Billone, Paul S.; Johnson, Paul A.; Lin, Shuqiong; Scaiano, J. C.; DiLabio, Gino A.; Ingold, K. U.

This publication could be one of several versions: author's original, accepted manuscript or the publisher's version. / La version de cette publication peut être l'une des suivantes : la version prépublication de l'auteur, la version acceptée du manuscrit ou la version de l'éditeur.

For the publisher's version, please access the DOI link below. / Pour consulter la version de l'éditeur, utilisez le lien DOI ci-dessous.

Publisher's version / Version de l'éditeur:

<https://doi.org/10.1021/jo1021794>

The Journal of Organic Chemistry, 76, 2, pp. 631-636, 2010-12-23

NRC Publications Record / Notice d'Archives des publications de CNRC:

<https://nrc-publications.canada.ca/eng/view/object/?id=f935bff7-76d4-498c-8cff-27f029fe69be>

<https://publications-cnrc.canada.ca/fra/voir/objet/?id=f935bff7-76d4-498c-8cff-27f029fe69be>

Access and use of this website and the material on it are subject to the Terms and Conditions set forth at

<https://nrc-publications.canada.ca/eng/copyright>

READ THESE TERMS AND CONDITIONS CAREFULLY BEFORE USING THIS WEBSITE.

L'accès à ce site Web et l'utilisation de son contenu sont assujettis aux conditions présentées dans le site

<https://publications-cnrc.canada.ca/fra/droits>

LISEZ CES CONDITIONS ATTENTIVEMENT AVANT D'UTILISER CE SITE WEB.

Questions? Contact the NRC Publications Archive team at

PublicationsArchive-ArchivesPublications@nrc-cnrc.gc.ca. If you wish to email the authors directly, please see the first page of the publication for their contact information.

Vous avez des questions? Nous pouvons vous aider. Pour communiquer directement avec un auteur, consultez la première page de la revue dans laquelle son article a été publié afin de trouver ses coordonnées. Si vous n'arrivez pas à les repérer, communiquez avec nous à PublicationsArchive-ArchivesPublications@nrc-cnrc.gc.ca.



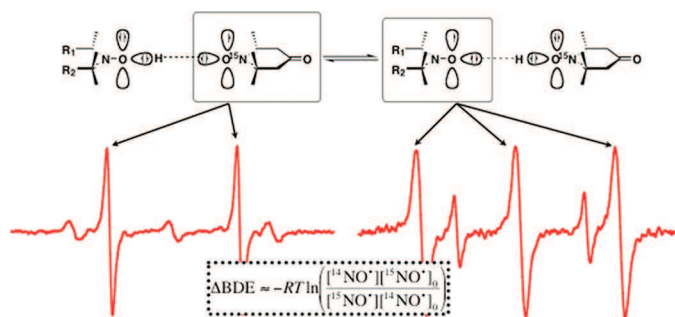
Accurate O–H Bond Dissociation Energy Differences of Hydroxylamines Determined by EPR Spectroscopy: Computational Insight into Stereoelectronic Effects on BDEs and EPR Spectral Parameters

Paul S. Billone,^{*,†} Paul A. Johnson,[‡] Shuqiong Lin,[§] J. C. Scaiano,[†] Gino A. DiLabio,^{*,‡} and K. U. Ingold[§]

[†]Department of Chemistry, University of Ottawa, 10 Marie Curie, Ottawa, ON, Canada K1N 6N5,
[‡]National Institute for Nanotechnology, National Research Council of Canada, 11421 Saskatchewan Drive, Edmonton, AB, Canada T6G 2M9, and [§]National Research Council, 100 Sussex Drive, Ottawa, ON, Canada K1A 0R6

paulb@photo.chem.uottawa.ca; gino.dilabio@nrc-cnrc.gc.ca

Received November 3, 2010



Differences in O–H bond dissociation enthalpies (Δ BDEs) between the hydroxylamine of ^{15}N -labeled TEMPONE and 10 *N,N*-di-*tert*-alkyl hydroxylamines were determined by EPR. These Δ BDEs, together with the g and a^{N} values of the derived nitroxide radicals, are discussed in relation to various geometric, intramolecular dipole/dipole, and steric effects and in relation to the results from DFT calculations. We find that dipole/dipole interactions are the dominant factors in dictating a^{N} values and O–H BDEs in all of these structurally similar nitroxides and hydroxylamines, respectively. The importance of including the Boltzmann distribution of conformations for each nitroxide in the a^{N} calculations is emphasized.

Introduction

As applications for hydroxylamines continue to be discovered and vigorously pursued, it is increasingly important to be able to predict and understand their reactivities. For instance, the utility of hydroxylamines as oxidation catalysts is critically dependent on their O–H bond dissociation enthalpies (BDEs).^{1,2} The key step in such reactions is H-atom transfer (HAT) from the substrate to the derived nitroxide radical, which is favored when the BDE of the substrate C–H

bond is comparable to or lower than the hydroxylamine's O–H BDE. The prediction of O–H BDEs and BDE differences (Δ BDEs) is important when selecting effective hydroxylamine catalysts.³ We propose that the subtle effects on the hydroxylamine O–H BDEs examined herein serve as a basis for the development of more comprehensive and accurate computational models since a reliable model should be able to account for both the large and small effects in BDE calculations.

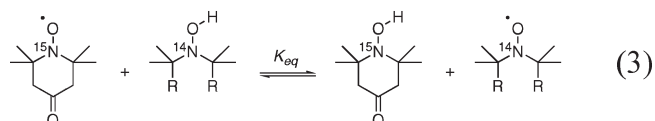
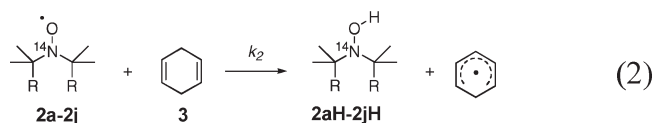
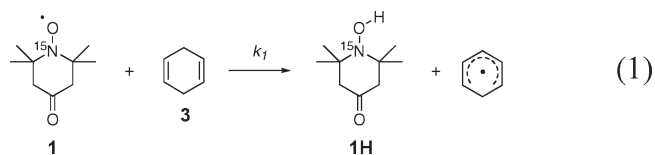
An EPR radical equilibration technique was used to determine accurate Δ BDEs for hydroxylamines yielding

(1) Amorati, R.; Lucarini, M.; Mugnaini, V.; Pedulli, G. F.; Minisci, F.; Recupero, F.; Fontana, F.; Astolfi, P.; Greci, L. *J. Org. Chem.* **2003**, *68*, 1747–1754.

(2) Coseri, S.; Mendenhall, G. D.; Ingold, K. U. *J. Org. Chem.* **2005**, *70*, 4629–4636.

(3) Chong, S.-S.; Fu, Y.; Liu, L.; Guo, Q.-X. *J. Phys. Chem. A* **2007**, *111*, 13112–13125.

SCHEME 1. Irreversible Reduction of Nitroxides by 1,4-Cyclohexadiene (eqs 1 and 2) and Hydrogen-Atom Transfer Equilibrium between Nitroxides and Hydroxylamines (eq 3)



stable nitroxide radicals in *n*-heptane, a nonpolar, nonpolarizable, non-hydrogen bond acceptor (non-HBA), and non-HB donor (non-HBD) solvent, thus ensuring that the Δ BDEs required no correction for solvent effects (which are particularly large for O–H BDEs).^{4–6} This solvent also ensured that the nitroxides' N hyperfine coupling constants (hfcc, a^N) were also free of otherwise very large solvent effects.^{7,8} Δ BDE values were determined with respect to that of ¹⁵N-labeled 2,2,6,6-tetramethylpiperid-4-one-1-hydroxyl (**1H**) because the ¹⁵N-labeled nitroxide (**1**) is commercially available. The O–H BDE of **2aH** was determined to be 71.8 kcal/mol by calorimetry in 1973.⁹ However, this value must be revised downward by 1.2 kcal/mol to 70.6 kcal/mol (–1.1 kcal/mol because of a revised heat of formation of *E*-azobenzene,¹⁰ plus a –0.1 kcal/mol correction for HB effects^{10,11}).

Results

Reduction of Nitroxide Radicals by 1,4-Cyclohexadiene.

The slow, irreversible reduction of nitroxides by 1,4-cyclohexadiene, **3** (Scheme 1, eqs 1 and 2), was exploited to determine the equilibrium constant, K_{eq} , for hydrogen atom transfer (HAT) between the nitroxide/hydroxylamine couples **1/1H** and **2x/2xH** (eq 3; the ¹⁵N gives **1** a 2-line EPR spectrum that is readily distinguished from the 3-line spectra of ¹⁴N-nitroxides, **2**). Diene **3** was chosen as the *in situ* reducing agent because the cyclohexadienyl radical is rapidly oxidized to benzene by a second nitroxide, which makes reactions 1 and 2 irreversible.¹² In addition, **3** and

benzene are both very weak HBAs.¹³ The reaction of **1** with excess **3** follows first-order kinetics, and the reaction is also first-order in **3** (Figure S1 in Supporting Information). The second-order rate constant for the **2a** + **3** (\equiv **1** + **3**) reaction, k_1 , corrected for the 2:1 stoichiometry, is $3.5 \times 10^{-5} \text{ M}^{-1} \text{ s}^{-1}$ at 21 °C.

Measurement of K_{eq} for Nitroxide/Hydroxylamine Reactions. Under pseudo-first-order conditions with respect to **3**, K_{eq} can be written as

$$K_{eq} = \frac{[^{15}\text{NO-H}][^{14}\text{NO}^*]}{[^{15}\text{NO}^*][^{14}\text{NO-H}]} = \frac{[^{14}\text{NO}^*][^{15}\text{NO}^*]_0(1 - e^{-k_1[3]t})}{[^{15}\text{NO}^*][^{14}\text{NO}^*]_0(1 - e^{-k_2[3]t})} \quad (4)$$

At long times, eq 4 simplifies to

$$K_{eq} = \frac{[^{14}\text{NO}^*][^{15}\text{NO}^*]_0}{[^{15}\text{NO}^*][^{14}\text{NO}^*]_0} \quad (5)$$

Measurement of the ¹⁵N/¹⁴N ratio (by double integration of the corresponding EPR signals) before addition of **3** and following equilibration¹⁹ after its addition yielded K_{eq} for each **2x/2xH** and **1/1H** pair. The very slow reduction by **3** compared to the rates of the forward and reverse reactions²⁰ in eq 3 allowed for the use of eq 5 while using low starting concentrations of nitroxides (see Experimental Section). The values of K_{eq} so obtained correspond to the differences in free energies for each pair, ΔG . These quantities yield Δ BDEs (eq 6) for the O–H bonds of the corresponding hydroxylamines based on the assumption that $\Delta S = 0$ for **3**.²¹ This assumption is reasonable considering that the measurements were made in solvents that are neither hydrogen-bond-donating nor -accepting.²² Equilibrium constants for reaction 3 with 10 **2x/2xH** couples are presented in Table 1. Errors are the standard deviation from a minimum of three separate experiments (see Experimental Section for details). For the near-identity reaction between **1/1H** and **2a/2aH**, $K_{eq} = 1.00 \pm 0.05$, a result that validates our experimental procedure because no significant N-isotope effect would be expected. Values of K_{eq} for the **1/1H** and nine **2x/2xH** ($x = \text{b–j}$) pairs were all greater than 1.0,

(13) Abraham, M. H.; Grellier, P. L.; Prior, D. V.; Morris, J. J.; Taylor, P. J. *J. Chem. Soc. Perkin Trans. 2* **1990**, 521–529.

(14) Frisch, M. J., et al. *Gaussian 03*, D.01; Gaussian, Inc.: Wallingford, CT, 2004.

(15) Becke, A. D. *J. Chem. Phys.* **1993**, *98* (7), 5648–5652.

(16) Lee, C. T.; Yang, W. T.; Parr, R. G. *Phys Rev B* **1988**, *37* (2), 785–789.

(17) Barone, V., Structure, Magnetic Properties and Reactivities of Open-Shell Species from Density Functional and Self-Consistent Hybrid Methods. In *Recent Advances in Density Functional Methods*; Chong, D. P., Ed.; World Scientific: Singapore, 1995.

(18) See ref 37 of Foti, M. C.; Daquino, C.; Mackie, I. D.; DiLabio, G. A.; Ingold, K. U. *J. Org. Chem.* **2008**, *73*, 9270–9282.

(19) Note that this equilibration refers to the time it takes for the nitroxide/hydroxylamine bimolecular reaction to establish equilibrium. The ratio $[^{14}\text{NO}]/[^{15}\text{NO}]$ was measured periodically for each experiment until it became constant.

(20) Wu, A.; Mader, E. A.; Datta, A.; Hrovat, D. A.; Borden, W. T.; Mayer, J. M. *J. Am. Chem. Soc.* **2009**, *131*, 11985–11997.

(21) See also: Lucarini, M.; Pedulli, G. F.; Cipollone, M. *J. Org. Chem.* **1994**, *59*, 5063–5070.

(22) A referee has suggested that conformational entropy may result in ΔS in **3** that is not strictly zero. We believe that the effects of conformational flexibility will likely cancel in cases where **3** describes H exchange between two six-membered rings. However, this assumption may break down in the exchange between **2aH** and the five-membered rings, **2h** and **2i**, and with **2j**.

(4) Wayner, D. D. M.; Luszyk, E.; Pagé, D.; Ingold, K. U.; Mulder, P.; Laarhoven, L. J. J.; Aldrich, H. S. *J. Am. Chem. Soc.* **1995**, *117*, 8737–8744.

(5) Snelgrove, D. W.; Luszyk, J.; Banks, J. T.; Mulder, P.; Ingold, K. U. *J. Am. Chem. Soc.* **2001**, *123*, 469–477.

(6) Pratt, D. A.; Blake, J. A.; Mulder, P.; Walton, J. C.; Korth, H.-G.; Ingold, K. U. *J. Am. Chem. Soc.* **2004**, *126*, 10667–10675.

(7) Knauer, B. R.; Napier, J. J. *J. Am. Chem. Soc.* **1976**, *98* (15), 4395–4400.

(8) Beckwith, A. L. J.; Bowry, V. W.; Ingold, K. U. *J. Am. Chem. Soc.* **1992**, *114*, 4983–4992.

(9) Mahoney, L. R.; Mendenhall, G. D.; Ingold, K. U. *J. Am. Chem. Soc.* **1973**, *95*, 8610–8614.

(10) Mulder, P.; Korth, H.-G.; Pratt, D. A.; DiLabio, G. A.; Valgimigli, L.; Pedulli, G. F.; Ingold, K. U. *J. Phys. Chem. A* **2005**, *109*, 2647–2655.

(11) Astolfi, P.; Greci, L.; Paul, T.; Ingold, K. U. *J. Chem. Soc. Perkin Trans. 2* **2001**, No. 9, 1631–1633.

(12) Doba, T.; Ingold, K. U. *J. Am. Chem. Soc.* **1984**, *106*, 3958–3963.

TABLE 1. Equilibrium Constants (K_{eq} , in *n*-Heptane at 21 °C) for Some Di-*tert*-alkyl Hydroxylamines and O–H Δ BDEs ($2xH - 1H$, cal mol⁻¹)

Compound	Structure	K_{eq}	Δ BDE ^a
2aH		1.00 ± 0.05	0 ± 28 (0/0) ^b
2bH		2.46 ± 0.38	-530 ± 90 (-1084/-1387)
2cH		1.55 ± 0.15	-260 ± 60 (-812/-1062)
2dH		2.19 ± 0.32	-460 ± 80
2eH		2.09 ± 0.15	-420 ± 40 (-1025/-1257)
2fH		1.36 ± 0.31	-180 ± 130
2gH		1.05 ± 0.07	-30 ± 40
2hH		17.5 ± 1.3	-1670 ± 40
2iH		13.6 ± 1.8	-1520 ± 80 (-2965/-3608)
2jH		14.2 ± 4.9	-1550 ± 200 (-2087/-2302)

^aMeasured (eq 6) and, in brackets, Δ BDEs calculated using Gaussian-03¹⁴ with (left) B3¹³LYP¹⁶/EPR-III¹⁷//B3LYP/6-311+G(d,p) and (right) extrapolated CCSD.¹⁸ These data were obtained using Boltzmann-averaged enthalpies for both parents and radicals. ^bCalculated absolute O–H BDE for **2aH** are 64.8 (B3LYP) and 71.8 (CCSD) kcal mol⁻¹. Absolute O–H BDEs for **2bH**–**2jH** should be based on Δ BDEs and a **2aH** BDE = 70.6 kcal/mol, see text.

indicating that the O–H bond in **1H** is stronger than those in **2bH**–**2jH**.

$$\Delta\text{BDE} \approx \Delta(\Delta G) = -RT \ln K_{eq} \quad (6)$$

Measurement of Nitroxide ESR Spectroscopic Parameters. Isotropic values of g and a^N are presented in Table 2. These values were calibrated using the third and fourth lines of the Mn²⁺ signal of a solid standard Mn probe. Among the commercially available piperidinyl-*N*-oxyls (**2a**–**2e**), **2a** has the smallest g value and the smallest a^N value, and **2aH** has the largest O–H BDE. Computed spin-densities reveal that the O-atom of the nitroxide moiety carries a greater spin density in **2a** than in **2b**–**2e**. Because hybridization of the 4-carbon (i. e., sp² in **2a/2aH** vs sp³ in **2b/2bH**–**2e/2eH**) might play a role in

determining the g , a^N , and O–H BDE values in these compounds, radicals **2f** and **2g** were synthesized by a reported procedure.^{23,24} Both **2fH** and **2gH** were found to have O–H BDEs closer to that of **2aH** than to those of **2bH**–**2eH**, though the a^N values of **2f** and **2g** (and the computed spin density on the O atom of the NO[•] moiety of **2f**) are more comparable to those of **2b**–**2e** than **2a**. It would appear, therefore, that an exocyclic double bond at the 4-position strains the piperidine ring and causes the O–H BDEs of **2aH**, **2fH**, and **2gH** to be larger than those for **2bH**–**2eH**. However, the 4-C atom's hybridization, by itself, does not explain why, for example, the O–H BDEs for **2bH**–**2eH** are not equal, nor does it totally account for the relative conformational stability of chair and twist-boat structures (Table 2).

DFT Calculations. To gain a greater insight into the effects of structure on the O–H BDEs and on the g and a^N values, density-functional theory calculations were performed on **2a**–**2f** and **2h**–**2j** (see footnotes a in Tables 1 and 2). These calculations predict that **2a** exists in two conformations at room temperature, 41.4% chair (ch) and 58.6% twist-boat (tb) (see Figure 1), the latter corresponding to the reported X-ray structure.²⁷ In contrast, **2b** exists primarily (99.3%) in a chair conformation. The **2a**-ch and **2a**-tb conformations have different geometries around the N-atom and therefore different conjugation in the N–O groups. Specifically, the N-atom in **2a**-ch has more sp³ character than the N-atom in **2a**-tb, as can be seen from the out-of-plane angle associated with the N–O bond relative to the plane defined by the CNC atoms, viz., 21.7° (ch) and 0° (tb), respectively (see Table 2). Spin-delocalization from O to N is favored by small θ values and is extremely sensitive to small changes in conjugation (vide infra). For example, the computed unpaired spin density on the O- and N-atoms in **2a**-ch are 0.501 and 0.437, respectively, whereas in **2a**-tb these values are 0.482 and 0.485, respectively. Conjugative delocalization of the unpaired electron onto the N-atom of **2a** is reduced by the opposing local N–O and C=O dipoles to an extent that depends on their alignment. The large contribution from the twist-boat conformation that has its N–O[•] and C=O bond vectors nearly collinear but with opposed dipoles (Figure 1) causes the value a^N to be appreciably smaller in **2a** than in **2b** (both by experiment and calculation, Table 2).

Spin is more localized on the O-atom of the NO[•] group in **2a** than in **2b**, and this will contribute to the larger O–H BDE found for **2aH** than for **2bH**. Furthermore, BDE calculations (B3LYP) for the process **2aH** → **2a**-ch[•] + H[•] yields an O–H BDE that is 132 cal mol⁻¹ larger than that obtained using Boltzmann-averaged enthalpies. This analysis suggests that dipole/dipole interactions in the hydroxylamine and its nitroxide may have a greater influence on O–H BDEs than does the presence of twist-boat conformations in the Boltzmann distribution of radicals. Such intramolecular dipole/dipole forces also nicely explain why the O–H BDE in **2bH** is weaker

(23) Kalai, T.; Szabo, Z.; Jeko, J.; Hideg, K. *Org. Prep. Proced. Int.* **1996**, *28*, 443–452.

(24) Several attempts to synthesize the unknown 4-vinyl-TEMPO were unsuccessful.

(25) Hamprecht, F. A.; Cohen, A. J.; Tozer, D. J.; Handy, N. C. *J. Chem. Phys.* **1998**, *109*, 6264–6271.

(26) Mackie, I. D.; DiLabio, G. A. *J. Phys. Chem. A* **2008**, *112* (43), 10968–10976.

(27) Bordeaux, D.; Lajz rowicz, J. *Acta Crystallogr., Sect. B* **1974**, *30*, 790–792.

TABLE 2. Measured EPR Parameters for Nitroxides **2a–2j** in *n*-Heptane at 21 °C and Calculated a^N Values^a plus Calculated Percentage of Populations of Structures Having a Chair Conformation and the Spin Density on the O- and N-Atoms

nitroxide	<i>g</i>	$a_{\text{exp}}^N/\text{G}$	$a_{\text{calc}}^N/\text{G}$	% chair ^b	θ^c	N spin density ch/tb	O spin density ch/tb
2a	2.00574(2)	14.24	13.78	41.4	0.0 ^d	0.437/0.485	0.501/0.482
2b	2.00586(8)	15.30	15.37	99.3	21.8	0.451/0.493	0.493/0.476
2c	2.00587(7)	15.18	15.21	99.1	21.8	0.452 ^e /0.491 ^f	0.493 ^e /0.478 ^f
2d	2.00583(2)	15.12	15.25	98.7	21.6	0.455 ^e /0.492 ^f	0.491 ^e /0.476 ^f
2e	2.00584(3)	15.22	15.28	99.6	21.7	0.458 ^e /0.492 ^f	0.490 ^e /0.476 ^f
2f	2.00590(1)	15.04	14.87	85.0	21.7	0.450 ^e /0.496 ^f	0.494 ^e /0.475 ^f
2g	2.00593(9)	15.17	<i>g</i>	<i>g</i>	<i>g</i>	<i>g</i>	<i>g</i>
2h	2.00557(4)	13.85	12.71		4.0	0.480 ^{h,i}	0.479 ^{h,i}
2i	2.00561(5)	13.72	12.65		6.6	0.476 ^{h,i}	0.483 ^{h,i}
2j	2.00574(8)	15.17	15.28		19.7	0.478 ^h	0.489 ^h

^aBoltzmann-averaged from structures obtained using B971²⁵/6-31+G(d,p) with dispersion-correcting potentials.²⁶ ^bCalculated only for the piperidinylnitroxyl species. ^cThe out-of-plane angle of the N–O• bond relative to the plane defined by the C–N–C atoms for the most stable conformer. ^dThis value corresponds to the twist-boat structure, which is the most enthalpically stable conformer; the chair structure angle is 21.7°. ^eAverage value of all chair conformations. ^fAverage value of all twist-boat conformations. ^gTechnical difficulties prevented calculations on this radical. ^hThese structures do not have chair or twist-boat conformations. ⁱAverage value of multiple conformations.

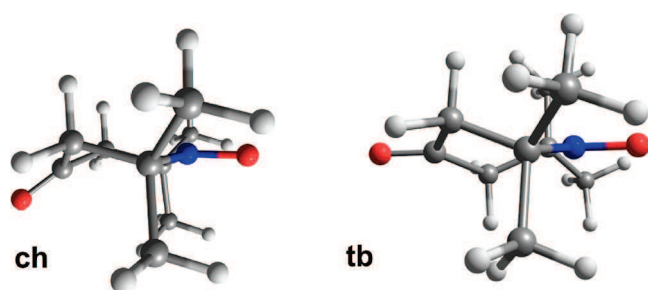


FIGURE 1. Optimized **2a** chair (ch) is predicted to be 0.2 kcal/mol higher in enthalpy than the **2a** twist-boat (tb). The calculated barrier for the **2a**-ch and **2a**-tb interconversion is ca. 2.6 kcal/mol.

than in **2cH–2eH** (all of which have inductively electron-withdrawing groups at the 4-position). Of course, both intramolecular dipole/dipole forces and Boltzmann distributions of conformations should be considered when comparing a^N values (vide infra). Note that both of the theoretical methods we used are unable to reproduce small differences in BDE in the nitroxides. Therefore, the calculated O–H BDEs should be considered with caution.²⁸

The effect of non-ground state conformations on a^N (**2b–2i**) is illustrated in Figure 2a where the measured values have been plotted against values calculated for the lowest enthalpy conformations of the nitroxides.²⁹ There is a fairly good correlation, and for the six-membered cyclic nitroxides, **2a–2f**, there are only two outliers, **2a** and **2f**, both of which have conformational excited state structures that account for a significant fraction of their populations at room temperature. These deviations arise because of significant differences in a^N for the chair and twist-boat conformations, e.g., $a^N(\mathbf{2a}\text{-ch})_{\text{calc}} = 15.29$ G and $a^N(\mathbf{2a}\text{-tb})_{\text{calc}} = 12.72$ G.³⁰ Boltzmann averaging a^N values for all of the calculated conformers greatly improves the relationship between calculation and

(28) The O–H BDEs presented in Table 1 indicate that both DFT and wave function theory fail to reflect accurately the small, subtle differences observed experimentally. Both B3LYP and CCSD predict the observed trends in ΔBDE , with the former method giving better agreement with experiment.

(29) For the piperidine nitroxides, the lowest enthalpy conformation is a chair in all cases except **2a**.

(30) The average calculated a^N (G) values for chair/twist-boat conformations are **2a** 15.29/12.72, **2b** 15.38/12.93, **2c** 15.26/12.88, **2d** 15.28/12.89, **2e** 15.29/12.91, **2f** 15.24/12.79. These were obtained by Boltzmann averaging separately over chair and twist-boat structures.

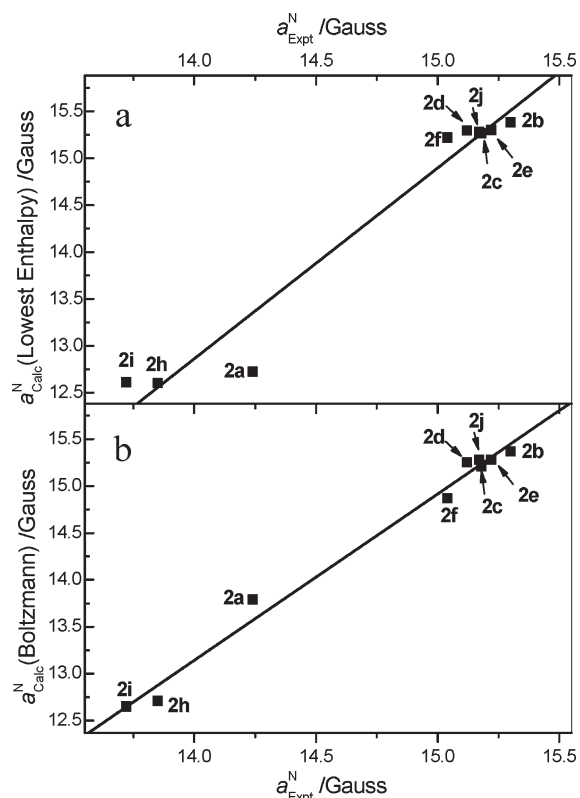


FIGURE 2. Plots of calculated versus experimental a^N values. (a) Values calculated for the lowest enthalpy conformers; $r^2 = 0.958$, $\text{SD} = 0.29$ G. (b) Values obtained by Boltzmann-averaging all nitroxide conformers; $r^2 = 0.989$, $\text{SD} = 0.13$ G.

experiment (see Figure 2b). The five-membered ring nitroxides, **2h** and **2i**, also have several conformations. For example, **2h** has low enthalpy pseudoequatorial (**2h-a**) and pseudoaxial (**2h-b**) conformations (see Figure 3). These structures differ in enthalpy by 1.22 kcal mol⁻¹ and have significantly different a^N values. A structural analysis of the N–O moieties in the **2h** structures shows little difference in the hybridization of the N-center, which further emphasizes the influence of dipole–dipole forces on a^N values. The better correlation shown in Figure 2b relative to Figure 2a highlights the importance of Boltzmann averaging in calculating a^N values. However, the fact that the slope of the best-fit line in Figure 2b

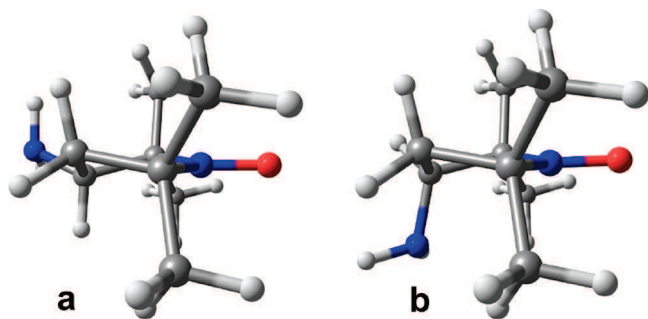


FIGURE 3. Optimized conformations for **2h**. (a) $a_{\text{calc}}^{\text{N}} = 12.60$ G. (b) $a_{\text{calc}}^{\text{N}} = 13.11$ G.

differs significantly from the expected value of 1 illustrates that there are still issues with the calculation of a^{N} values insofar as nitroxides **2a**, **2h**, and **2i** are concerned. That is, the experimental and calculated values of a^{N} for **2b–2f** and **2j** are in excellent agreement (see Table 2). For example, **2b** had a calculated a^{N} value of 15.37 G, which is very close to the experimental value of 15.30 G. We recently commented on the difficulties associated with calculating accurate hfcc's.³¹

Discussion

The pyrrolidine hydroxylamines, **2hH** and **2iH**, have O–H BDEs that are markedly lower than those of the piperidine hydroxylamines (Table 1). At first sight, the slightly lower g values for **2h** and **2i** compared with **2a–2g** might suggest greater unpaired spin localization on the N-atoms of the pyrrolidine-*N*-oxyls than on the N-atoms of the pyridinyl-*N*-oxyls. However, the lower a^{N} values for **2h** and **2i** compared with **2a–2g** would seem to indicate a smaller degree of unpaired spin localization on the N-atoms in **2h** and **2i**. These *apparently* contradictory indications about spin density location in five- and six-membered cyclic nitroxides are simply due to the different geometries of such rings, specifically their CNC angles, ca. 108° and 120°, respectively, and the effect this has on the N–O out-of-CNC-plane angle, θ , and the degree of s-character of the SOMO on the N atom. For example, DFT calculations reveal that the N–O bond is bent out of the plane defined by the C–N–C ring atoms by 4.0° in **2h**, whereas it is 21.8° in **2b** (see Table 2). What this means is that conjugative electron delocalization from the O-atom to the N-atom will be more favored in **2h** than in **2b**. This increased delocalization of unpaired spin density in **2h** and **2i** relative to **2b** is consistent with the calculated N–O bond lengths, which are smaller for the five- than for the six-membered rings, e.g., $R_{\text{N–O}}(\mathbf{2i}) = 1.277$ Å vs $R_{\text{N–O}}(\mathbf{2b}) = 1.286$ Å. The increased sp^3 character of the hybridization of the N in **2b** relative to the N in **2h** (and **2i**) results in a greater N hfcc in **2b**. In the case of **2j**, the N-atom has a significant degree of sp^3 character as evidenced by its large N–O out-of-CNC-plane angle and high a^{N} value (see Table 2). Thus some additional factor must be responsible for the low observed O–H BDE in **2jH**. We hypothesize that this factor is greater steric repulsion of the OH group in the hydroxylamine by the six flanking methyl groups in the more flexible acyclic architecture. In *o*-alkyl phenols, such steric repulsion is well established^{32,33} and is well-known to induce

an appreciable decrease in the O–H BDE on going from 2,6-dimethylphenol to 2,6-di-*tert*-butyl phenol (e.g., see Lucarini et al.³⁴).

The differences in the O–H BDEs of a variety of structurally similar hydroxylamines have been measured using a ¹⁵N-labeled nitroxide with unprecedented accuracy by a simple EPR equilibration technique. The observed trends in their O–H BDEs are rationalized on the basis of subtle dipole–dipole forces and other stereoelectronic effects that are also reflected in the spectroscopic properties of the corresponding nitroxide radicals. This work emphasizes the importance of exercising caution when using the a^{N} values of nitroxide radicals to glean information regarding the BDEs of the corresponding parent hydroxylamines. As the application of hydroxylamines in hydrogen atom transfer-assisted catalysis continues to develop, researchers must look beyond the spectroscopic properties of the nitroxide species to assist in the rational design of new nitroxide catalysts and to gain insight into their catalytic mechanisms. These subtle differences are a challenge to modern computational theory, whose methods must be modified in order to account for these small effects before it can be used for computational catalyst screening.

Experimental Section

Materials and Instrumentation. Nitroxide **1** was purchased from C/D/N Isotopes; nitroxides **2a**, **2b**, **2c**, **2e**, and **2i** were purchased from Sigma-Aldrich; nitroxide **2d** was purchased from Alfa Aesar; nitroxide **2h** was purchased from Acros Organics; nitroxide **2j** was purchased from Eastman Kodak. In all cases, the highest purity available nitroxide was purchased and used as received. Nitroxides **2f** and **2g** were synthesized by a reported procedure.²³ 1,4-Cyclohexadiene (**3**) was run through a plug of silica immediately before use to remove the dihydroquinone (DHQ) stabilizer.

All EPR spectra were recorded using a Jeol JES-FA100 equipped with a cylindrical TE011 resonator cavity. The third and fourth resonance lines of a solid-state Mn^{2+} probe inserted directly into the resonator were used to calibrate a^{N} and g values. All samples were recorded without a temperature controller unit, but cavity temperature was constant at 21 ± 1 °C as measured by a thermocouple inserted into the resonator between sample measurements. Double integration for concentration determination was performed by integrating the same magnetic field interval across all replicate samples.

Kinetics of Reduction of 2a by 3. A vial of 2 mL freshly purified 1,4-cyclohexadiene, **3**, was purged with N_2 for 20 min, and 500 μL was transferred by hypodermic syringe into a septum sealed, nitrogen-filled, EPR tube. The tube was placed into the EPR, and the cavity was tuned. Five microliters of a 2.7 mM stock solution of **2a** in heptane was added directly to the solution and EPR spectra (10 s sweep time) were recorded at 14 s intervals for 2000 measurements. The logarithm of the peak-to-peak heights of the first nitroxide peak in the as-obtained spectra were plotted vs time and fit to a linear equation (Figure S1, Supporting Information). Using the concentration of neat **3** as 10.7 M, a bimolecular rate constant of $3.5 \times 10^{-5} \text{ M}^{-1} \text{ s}^{-1}$ was obtained upon correction for the 2:1 stoichiometry (vide supra) of the reduction reaction.

K_{eq} Measurements. This procedure is illustrated for the measurement of K_{eq} of the **1H/2e** couple, but all other values were determined by the same method.

(31) DiLabio, G. A.; Ingold, K. U. *Can. J. Chem.* **2010**, *88*, 1053–1056.
 (32) Ingold, K. U.; Taylor, D. R. *Can. J. Chem.* **1961**, *39* (3), 471–480.
 (33) Ingold, K. U. *Can. J. Chem.* **1962**, *40* (1), 111–121.

(34) Lucarini, M.; Pedrielli, P.; Pedulli, G. F.; Cabiddu, S.; Fattuoni, C. *J. Org. Chem.* **1996**, *61*, 9259–9263.

A solution of 1.3×10^{-5} M of **1** and 2.9×10^{-5} M of **2e** was prepared in 2.0 mL of heptane, and 500 μ L was transferred to each of three EPR tubes. The tubes were sealed with a septum and purged by bubbling with Ar for 30 min using long SS syringe needles. An EPR spectrum was run of each tube, and the relative concentrations of radicals **1** and **2e** were calculated by double-integration of the easily distinguishable low-field lines of the radicals and multiplication by 2 and 3, respectively. Using a microliter syringe with a 20 cm needle, 5 μ L of **3**, freshly purified as described above, was added directly through a rubber septum to each solution, and the septa were wrapped with parafilm. EPR spectra were recorded until the relative concentrations of the two radical species were constant between two measurements separated by at least 2 h, indicating that equilibrium had been reached (about 60–70 h). K_{eq} was then calculated for each tube according to eq 5. This entire procedure was then repeated a second time on a different

day using freshly prepared solutions of **1** and **2e**. The K_{eq} value reported in Table 1 is the calculated mean value of all 6 samples and errors were calculated as σ .

Acknowledgment. We thank Dr. Vincent Maurel and Robert Godin for helpful discussion and technical assistance. P.A.J., P.S.B., and J.C.S. acknowledge financial support from the Natural Sciences and Engineering Research Council of Canada (NSERC); P.S.B. and J.C.S. acknowledge support from CFI and the Government of Ontario.

Supporting Information Available: Kinetics of reduction of **2a** by **3**; Cartesian coordinates for optimized structures from calculations. This material is available free of charge via the Internet at <http://pubs.acs.org>.